Nuclear Instruments and Methods in Physics Research A 1076 (2025) 170488

Contents lists available at ScienceDirect

Nuclear Inst. and Methods in Physics Research, A

journal homepage: www.elsevier.com/locate/nima

Full Length Article

Optical characterization of UV-transmitting acrylics for the Hyper-Kamiokande multi-PMT module

Alan Cosimo Ruggeri [a,*], Riccardo Funari [b], Deborah Katia Pallotti [c], Antonio Di Nitto [a,d], Bartolomeo Della Ventura [d], Aurora Langella [a,d], Lucas Nascimiento Machado [e], Davide Bianco [a,f], Luigi Lavitola [a,d], Alfonso Boiano [a], Alessandro Di Nola [a,d], Maria De Luca [d], Ciro Riccio [g], Raffaele Velotta [a,d], Pasqualino Maddalena [a,d], Gianfranca De Rosa [a,d]

[a] Istituto Nazionale di Fisica Nucleare, Sezione di Napoli, Via Cintia, Napoli, 80126, Italy
[b] Scuola Superiore Sant'Anna Institute of Mechanical Intelligence, Via G. Moruzzi, 1, Pisa, 56124, Italy
[c] Agenzia Spaziale Italiana (ASI), Matera Space Center, Località Terlecchia, snc, Matera, 75100, Italy
[d] Dipartimento di Fisica "Ettore Pancini", Università degli Studi di Napoli Federico II, Via Cintia, Napoli, 80126, Italy
[e] School of Physics and Astronomy, University of Glasgow, Glasgow, G12 8QQ, Scotland, United Kingdom
[f] Italian aerospace research centre (CIRA), Via Maiorise, snc, Capua (CE), 81043, Italy
[g] State University of New York at Stony Brook, Department of Physics and Astronomy, Stony Brook, NY, USA

ARTICLE INFO

Keywords:
Hyper-Kamiokande
Large-volume neutrino Cherenkov detector
Multi photomultiplier tube (mPMT)
Acrylic-material optical characterization
Neutrino oscillation experiment
Neutrino experiment

ABSTRACT

The Hyper-K project aims to construct a large-volume underground water Cherenkov detector to address unresolved questions in fundamental particle physics. The Hyper-Kamiokande far detector (HK) will incorporate various types of photodetectors, among which the multi-photomultiplier tube (mPMT) optical module providing critical directional information. To house the electronics and photodetectors, the mPMT vessel must meet specific criteria: (i) transparency in the visible and ultraviolet ranges, covering the spectrum of Cherenkov photons; (ii) an airtight seal to maintain optimal functionality in a dry, controlled environment; and (iii) resilience to the hydrostatic pressure of the HK water tank, which reaches 0.8 MPa. While glass has traditionally been used to fulfill these requirements, its intrinsic radioactivity may compromise the sensitivity of Hyper-K measurements. Acrylic that is transparent, impermeable and robust, by contrast, offers the advantage of a low-radioactivity. Optical characterizations were performed on various acrylic samples, revealing that optical performance is influenced not only by the material composition but also by the production processes used to achieve different thicknesses. Our findings support the use of acrylic as a viable alternative, but it is essential to rigorously monitor the material's performance during mass production to ensure optimal and uniform detector performance.

1. Introduction

Super-Kamiokande (SK) [1–3] is a 50-kton water Cherenkov detector located in the Kamioka mine in the Ikenoyama mountain in Japan, under about 1 km rock overhead (2.7 km water equivalent). It has been designed for advanced particle physics studies of neutrinos (e.g., proton decay, astrophysical and atmospheric neutrinos) and, since 2009, it also serves as a far detector for the Tokai to Kamioka (T2K) experiment for further investigation of neutrino oscillations and charge-parity (CP) violation [2]. SK data provided the confirmation of ν_μ-ν_e neutrino oscillation in 2013 [4]. Furthermore, excellent evidences of CP-violation in the lepton sector of the Standard Model have been reported by T2K through the investigation of the differences in oscillations between ν_μ-ν_e and $\bar{\nu}_\mu$-$\bar{\nu}_e$ [5]. Hyper-K is a next-generation water Cherenkov experiment, conceived on the success and experience of the T2K and SK experiments, implementing by using an enormous tank containing 258 kton of ultra-pure water hosting the Hyper-Kamiokande far detector (HK) [6,7].

In neutrino Cherenkov detectors, the Cherenkov light [8,9] generated by traveling charged particles stemming from neutrino interactions can be detected by photosensors (e.g., photomultiplier tubes (PMTs)). The configuration of these sensors plays a key role in optimizing light collection along the particle track in the detector and in enhancing

* Corresponding author.
E-mail address: acruggeri@na.infn.it (A.C. Ruggeri).

https://doi.org/10.1016/j.nima.2025.170488
Received 21 September 2024; Received in revised form 30 March 2025; Accepted 30 March 2025
Available online 16 April 2025

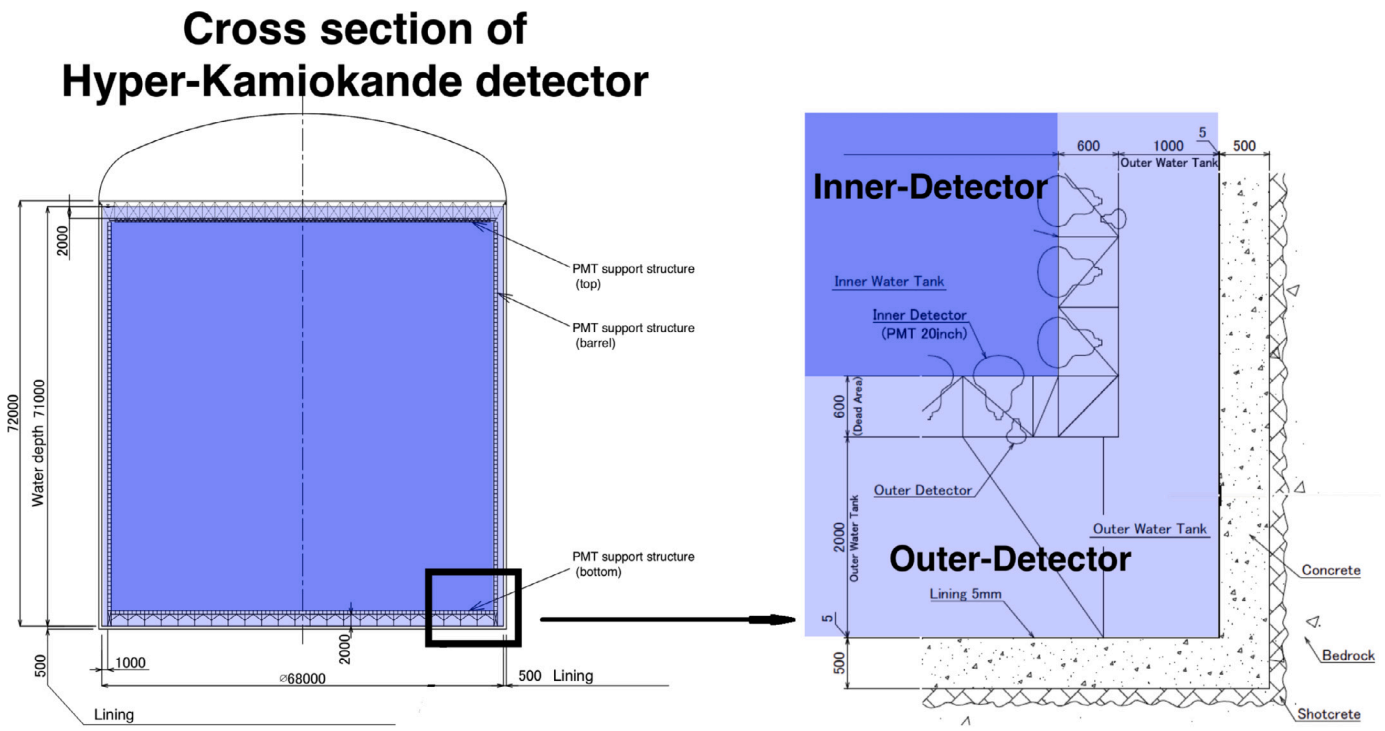

Fig. 1. Schematic of the cross section of the HK tank in the left panel, with in detail the detector frame and the wall of the cave in the right panel.
Source: Taken from Ref. [18]

reconstruction quality and background suppression. Detection of weak and rare events requires very high sensitivity and high accuracy in measurements of the particle trajectories, which motivates the construction of a new very large detector instrumented with a new suit of photodetection systems whose size will greatly exceed the dimensions of the largest current installations.

The detection volume system of HK will be divided into two main parts: the inner (ID) and the outer detectors (OD) as shown in Fig. 1. Both will consist of a large number of different types of photodetector sensitive elements. About 800 photodetectors in the ID will be based on the conceptual design of multi-PMT (mPMT) firstly introduced in the KM3NeT experiment [10]. The first prototype of the HK mPMT optical module, whose schematics are shown in Fig. 2, consists of a sealed pressure vessel instrumented with 19 3-inch PMTs, readout and all required power supplies electronics [11–13]. This elemental device will be used in conjunction with the 20-inch-diameter PMT type [14,15], consisting of a new version of the 20-inch-diameter PMT adopted for more than three decades in the SK detector [2,16]. In contrast to the 20-inch PMTs [17], the mPMTs are less sensitive to the Earth's magnetic field and are expected to provide better directional information [12].

While the ID will utilize mPMTs and 20-inch PMTs, each OD photosensor will consist of an alternative 3-inch PMT model along with a wavelength shifter plate. This arrangement involves positioning the wavelength shifter plate to face the exterior of the detector. The PMTs in the OD will serve as a veto system, enabling the identification of cosmic-ray muons entering the detector. For additional details on these detectors, refer to [19–23].

In the construction of water Cherenkov detectors a large effort is dedicated to define the structures hosting the photodetectors. Since they have to stand pressure of the surrounding water equal to 0.8 MPa, a protective sealed vessel able to withstand a pressure up to 1.26 MPa has been designed for safety reasons, in order to have water sealing and to guarantee reliable resistance, so that components inside will work in a dry environment for at least 20 years [24,25]. The protective case must guarantee excellent transparency to light in the ultraviolet (UV) range where the majority of Cherenkov photons are emitted, in accordance with a typical quantum efficiency of a PMT, namely between approximately 250–400 nm, also considering a very high transmittance at longer wavelength up to ~ 700 nm, which is characteristic of acrylic materials (e.g., [26]). Although glass or quartz are well suited for this purpose, the contamination of natural radioactive isotopes (e.g., ^{40}K, ^{226}Ra, ^{228}Ra, ^{235}U, ^{238}U and ^{232}Th) present in the standard production of such materials prevents their use in experiments attempting to study low-energy physics, such as Hyper-K; on the other hand, the employment of ultra-pure glass or quartz would rise the overall cost of the devices. Whereas acrylics present several advantages because it is a derivative of petroleum as relatively cheap cost, low intrinsic radioactivity, simple manufacture, impermeability to water, which in addition to their optical and mechanical properties, make them the most promising candidates. The upper limit contribution to the radiation of each detector element that would assure sensitivity to low energy neutrinos is reported in Table 1, and materials adopted for the construction of the 20-inch PMTs would respect these limits [27]. In this table, the radiation contribution of domes made in standard glass and acrylic material are reported as well. Clearly, the standard glass cannot be used to realize the mPMT dome.

Table 1
Radioactivity contributions, including key isotopes affecting the low-energy sensitivity of the Hyper-K detector. The upper radioactivity limit for the Hyper-K detection element is compared to the estimated radiation levels of theoretical mPMT domes made of standard glass and acrylic material. The total radioactivity contribution from the mPMT must remain below the indicated thresholds, which was achieved in the development of the 20-inch Hamamatsu R12860-HQE PMT model [27]. For both standard glass and acrylic materials, 10 mm-thick domes were assumed. Radioactivity measurements for standard glass and acrylic samples were conducted at the STELLA facility [28] at INFN Gran Sasso Laboratories.

	U-Chains (Bq)	Th-Chain (Bq)	^{40}K (Bq)
Upper limits	34.5	11.3	10.5
Stand. glass dome	85.2	18.4	11.5
Acrylic dome	$5 \cdot 10^{-4}$	$3 \cdot 10^{-4}$	$25 \cdot 10^{-4}$

Nowadays, acrylics are often used in neutrino and dark matter research as well, as light guide (e.g. MiniCLEAN [29]), as neutron shielding (e.g., the DEAP-3600 [30]), or as transparent vessels (e.g., Sudbury Neutrino Observatory [31], MiniCLEAN, Daya Bay [32] and the under-construction JUNO experiment [33]). Although the acrylic material is well suited for construction of complex detectors to be used in low-radioactive contamination environments in which high UV transmittance is required, it cannot be combined with acrylic glue as the latter may produce photoluminescence. Instead, the structural parts to assemble acrylic elements should be fabricated using different materials (e.g., steel, aluminium, screws, etc.). A series of tests on two acrylic brands with different thickness, and one acrylic glue with two different mixtures were performed, to verify their optical properties and select appropriate materials for the vessels of the HK mPMT photo-detection system. A detailed description of these tests is provided, including fluorescence analyses on the acrylic glue.

The paper is organized as follows, in Section 2 a description of the samples considered is given; Section 3 provides a description of the instrumentation used for transmittance, reflectance and photoluminescence measurements; Sections 4 and 5 are dedicated to detailed description of transmittance and reflectance results of the acrylic materials in different conditions, respectively; photoluminescence analyses of some glue samples are reported in Section 6; finally, we draw the conclusions in Section 7.

2. Samples preparation and description

Aiming at selecting the most suitable materials for the mPMT vessel implementation, the optical properties of eight samples of acrylic, one of optical gel and two samples of glues were studied in details. The first criterion to choose these acrylic samples consisted on a preliminary reference given by a commercial acrylic by the Kuraray Corporation[1], that was used in the SK experiment. Since its transmittance was known [34], this material was not included in our tests, but it was used as reference for an initial acrylic selection. Thus, after a selection among several commercial acrylics, based on their data sheets, the availability of the related companies, and the preliminary Hyper-K requirements regarding transmittance limits (Table 3), four acrylic samples with different thickness of the same "Plexiglass GS UVT" product by Evonik Industries AG[2] and other four samples with different thickness of the same "Polycast UVT" product by Poly One Corporation[3] were provided. These samples consist of sheets with different thickness cut by a mechanical saw in small squares of 55×55 mm^2 area (or less, concerning the tests with cuvette) to fit with the optical instruments. Based on the producer's indications and data sheets, all samples are ultraviolet transparent (UVT), a property essential to collect the Cherenkov light. A description of the samples is given in Table 2 and a picture of some samples is shown in Fig. 3. The companies provided acrylic sheets with surfaces already polished and with protective films applied on top of them. Then, at the INFN laboratory, the samples were prepared by cutting them along the sides not involved in transparency tests. Subsequently, after removing the protective films, the samples were placed inside the spectrometers.

The empty space between the acrylic and the PMT glass cover was filled with a suitable material to guarantee a proper optical and mechanical coupling. A crucial aspect for the selection of such material is its refractive index which has to match as much as possible to those of the acrylic dome and of the PMT photocathode cover borosilicate glass (i.e., ~ 1.49 and ~ 1.51, respectively, in the visible range). This choice reduces light reflections between the different media as discussed in Section 4. The gel WACKER SilGel® 612[4] has been selected as a good candidate for this task, with its nominal refractive index of 1.404 as reported in its data sheet, and because it is already used in the KM3NeT digital optical modules. It is comprised of two components that can be mixed within 1:1 and 1.5:1 ratios. We have opted for 1.5:1 ratio, in order to have a harder and less sticky layer. For the preparation of the gel, after the mixing of the two components, we followed a degassing procedure to remove air from the mixture and waited for about 24 h for a complete curing. The sample preparation consisted in pouring the liquid gel onto two dedicated acrylic surfaces prepared from the E5 mm and the P0187 original slices, and then let the gel cure for 24 h. The samples used in this procedure are shown in Fig. 4 and the thickness of gel in both samples is (5.0 ± 0.5) mm.

Table 2
Acrylic samples used for optical transmission and reflection tests. All samples are declared UV transmitting.

Company	Product name	Thickness (mm)	Sample name
Evonik	Plexiglas GS UVT	5	E5mm
		8	E8mm
		12	E12mm
		18	E18mm
Poly One	Polycast UVT	4.75	P0187
		6.35	P0250
		9.53	P0375
		12.70	P0500

Since the mPMT has to work underwater, a sealing closure is needed. A convenient design to resist external pressure and simplify sealing foresees two acrylic hemispheres united together in order to form a sphere; a picture and schematic drawings of the first preliminary prototype are shown in Fig. 5.

One of the options to unify the two hemispheres consists of using acrylic-based glues. However, some acrylic glues need to be cured by heating or UV irradiation, and these methods may damage PMTs and would be inapplicable, then we limited our glue tests on a brand which does not need heating or UV curing. Furthermore, for some brands of glue, UV light is absorbed and re-emitted back as visible light. This UV-induced visible fluorescence phenomenon can represent a source of background to the detection of UV Cherenkov light generated in neutrino interactions and, therefore, it was investigated for the ACRIFIX® 2R 0190[5], a two-component polymerization adhesive, satisfying the required tight sealing and suggested by Evonik that it uses to glue their acrylics. For its preparation, an amount ranging from 3% to 6% in weight of ACRIFIX® CA 0020 was added to ACRIFIX® 2R 0190, and stirred until no more striations were visible. During the mixing, air bubbles may rise to the surface of the adhesive, but they can be removed using a vacuum desiccator. We compared two samples: one prepared by the Evonik Company using a vacuum desiccator, and another prepared without a vacuum desiccator at the INFN laboratory in Naples, Italy. Fig. 6 shows a clear difference between these two samples, with the sample created at INFN being more opaque than the one from the Evonik labs. As mentioned, this difference may depend on the presence of air in the INFN sample and/or little differences in the proportion between the two glue components, but the essential point of our consideration is that the use of glue in the mPMT sealing closure will introduce further variables to control. A chemical procedure could be implemented, but compared to a mechanical approach, this latter minimizes potential risks and errors in the overall assembly. Mechanical components (such as screws, nuts, tools, and flanges) are significantly easier and cleaner to handle than chemical glues, which require, for instance, precise ingredient measurements, vapor control, mixing, and curing time.

[1] https://www.kuraray.com/company/overview

[2] http://corporate.evonik.com/, now Röhm Company https://www.roehm.com/en/

[3] http://www.polyone.com/

[4] https://www.wacker.com/h/en-us/silicone-rubber/silicone-gels/wacker-silgel-612-ab/p/000007546

[5] ACRIFIX® 2R 0190 Versatile - Reactive Cement

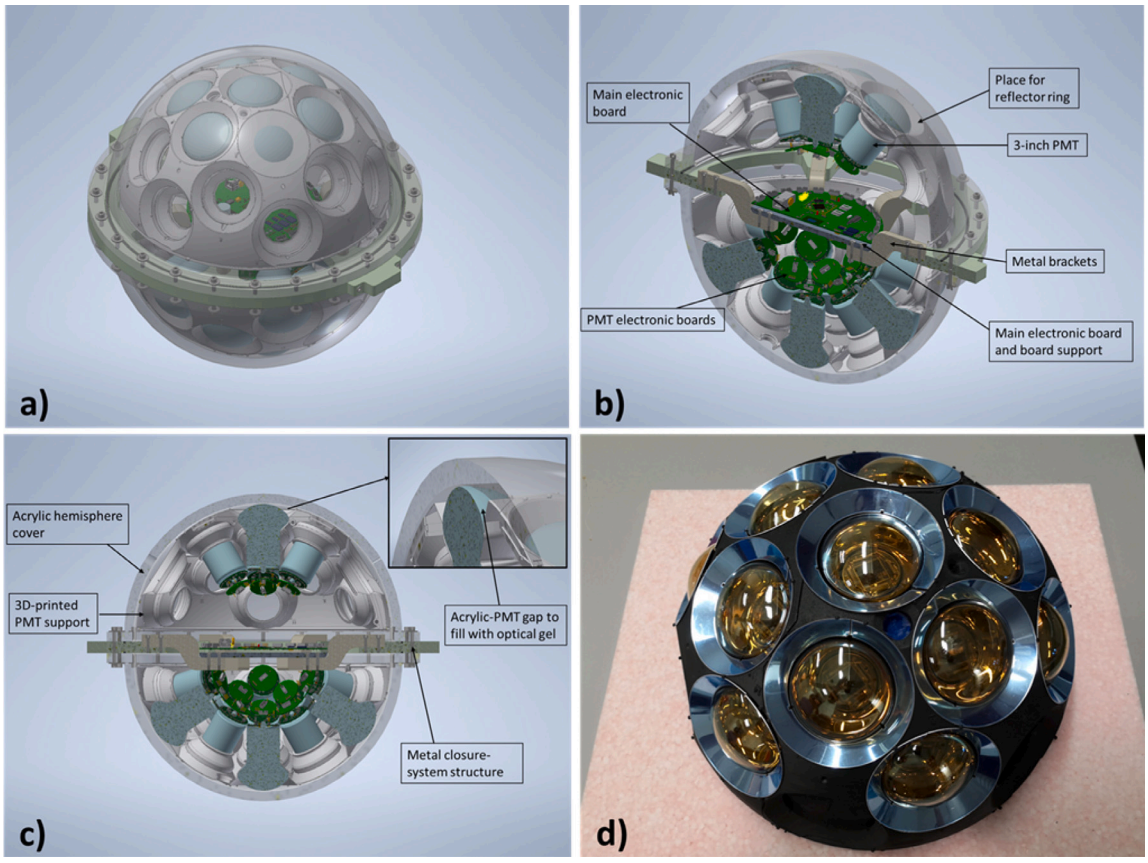

Fig. 2. In (a), (b) and (c), three schematic drawings of the first preliminary mPMT prototype. In (d), the assembly of the PMTs and reflector rings in the PMT support. The main components of the detector module are shown in (b) and (c), i.e, PMTs and their two PMT supports, the two acrylic hemispheres screwed to a metal ring as closure system, reflector rings to increase the reflective effective area to collect light, a layer of optical gel between PMTs and dome, and a plate fixed by brackets to place the electronic main board (more details in [24]).

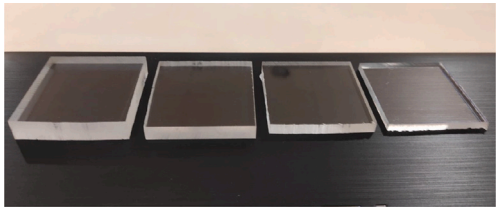

Fig. 3. Pictures of the Poly One samples after the 55 × 55 mm^2 cutting by saw. Same cuttings and shapes were done for the Evonik samples.

Fig. 4. Pictures of the acrylic samples with a 5 mm-thick optical-gel layer after its curing. Upon visual inspection, both samples appear transparent to visible light.

Fig. 5. Picture of the first preliminary mPMT prototype. The prototype is included in a white cage used to anchor the detector for sealing and operational tests performed at MEMPHYNO facility [35,36] at the APC Laboratory in Paris.

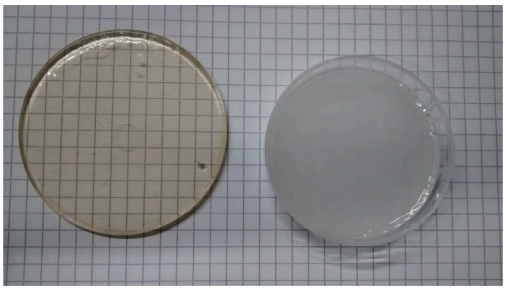

Fig. 6. ACRIFIX glue samples: (Left) sample prepared by Evonik Company; (Right) sample prepared at the INFN laboratory.

3. Experimental setup

We measured the transmittance and reflectance of the acrylic samples described in Section 2. Measurements in air have been repeated with two different spectrometers in order to perform a cross-check of the outcomes. Quartz cuvettes were used for the measurements in ultra-pure water. Finally, a layer of an optical gel coupled with the best selected acrylic samples has been analyzed and, in addition, photoluminescence analysis on a two-component acrylic glue was performed.

3.1. Instruments for transmittance and reflectance measurements

A Perkin Elmer Lambda 900 UV/Vis/NIR spectrometer was used for transmittance and reflectance measurements of each sample. The optical system scheme of this instrument with all details can be found in Ref. [37]. It consists of an all-reflecting double-monochromator optical system with very good resolution in wavelength between 185 nm and 3300 nm. This instrument produces a double beam so that samples and references are placed in their respective compartments (S and R positions, respectively) and their measurements are performed simultaneously using the same detector at equal light intensity per wavelength for better comparisons. Its wavelength accuracy is ± 0.08 nm in UV/Visible range and ± 0.32 nm in near infra-red (NIR) range, while its photometric accuracy is $\pm 0.08\%$ for transmittance and reflectance.

Two additional fixed-angle reflectance accessories with a 6° angle of incidence are placed in the S and R positions and used for reflectance measurements. An aluminium mirror is used as a reference in the R position, while the sample is placed in S. For the reference beam, i.e. the one reflected by the aluminium mirror, 100% reflectance is assumed, and the sample beam is compared with respect to this reference. Furthermore, the setup configuration is done to consider only the light of the first reflection of the sample surface if the sample is thicker than ~ 10 mm, but some fraction of the secondary reflection could be measured by the detector for thinner samples.

Additionally, transmittance measurements in pure water and with gel were performed with a 6715 UV/Vis spectrophotometer by Jenway. This spectrophotometer covers the UV and visible (Vis) wavelength ranging from 190 nm to 1100 nm with a pulsed xenon light source. Differently from the Perkin Elmer spectrometer, here the sample measurements are performed by using a single beam, comparing those with a reference measurement collected in a dedicated initial run. This reference run sets the 100% of the transmittance at all frequencies used for the measurement, hence all measurements on samples are compared relative to it. In other words, the transmittance of the sample under test are evaluated through these relative comparisons. Its wavelength accuracy is ± 0.1 nm, while its photometric accuracy is $\pm 0.5\%$.

A relevant aspect in performing these measurements is the cleaning of samples after they are cut during the preparation process. We observed a significant reduction in the transmittance through the cuvette filled with ultra-pure water when the non-cleaned acrylic samples were removed after a measurement. This can be due to acrylic microparticles resulting from the cutting process that are dispersed in water during the tests. For this reason, a proper sample cleaning procedure is imperative. Therefore, all the acrylic samples were sequentially cut, washed with abundant pure water and wiped with dust-free tissue paper.

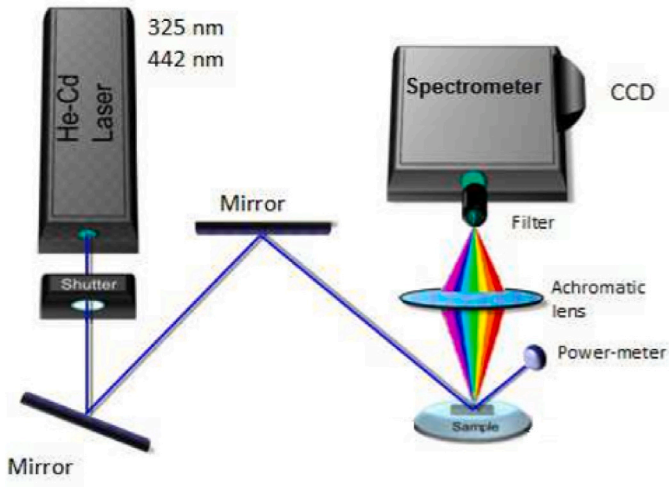

Fig. 7. Schematic of the photoluminescence setup used for the measurements.

3.2. Instruments for photoluminescence measurements

Room temperature continuous-wave photoluminescence measurements were performed by using as excitation source the two emission lines, $\lambda_1 = 325$ nm and $\lambda_2 = 442$ nm, of an HeCd laser. The laser was focused on the sample through a system of mirrors while the time duration of the sample excitation is controlled by an external shutter. Photoluminescence (PL) emissions are directed through an achromatic confocal lens system and an optical fiber to a 320 mm focal-length spectrometer coupled with Peltier–cooled CCD camera operating at -70 °C. Two high-pass filters from 365 nm and from 455 nm were used in order to avoid the acquisition of laser emission lines. A schematic of the PL setup is shown in Fig. 7.

4. Transmittance measurements

The main goal of this work is to identify the material with the largest transmittance (T) and lowest reflectance (R) among the selected samples in order to optimize light collection and to reduce light scattering by the vessel of the mPMT detection devices.

The ratio between the incoming (I_i) and outgoing (I_o) light intensities defines transmittance T:

$$T = \frac{I_o}{I_i}. \tag{1}$$

The outgoing intensity decreases with the increase of the medium thickness (s) as

$$I_o = I_i e^{-\alpha s}, \tag{2}$$

where α is the attenuation coefficient, which depends on the material properties and light wavelength. From Eqs. (1) and (2), T can be written as

$$T = e^{-\alpha s}, \tag{3}$$

hence, the transmittance explicitly depends on the properties and thickness of the medium. On the hand, in the experimental setup, light enters the medium after crossing an optically-discontinuous region corresponding to the boundary between acrylic and air or water, and

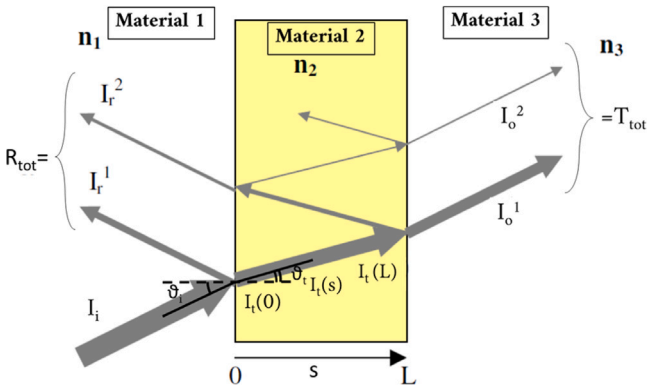

Fig. 8. The incoming light passes through the first n_1-n_2 discontinuity at $s = 0$, where it is partially reflected I_r^1 and transmitted $I_t(0)$. Part of $I_t(0)$ will be absorbed in the medium, reducing its intensity down to $I_t(L)$ at the n_2-n_3 boundary surface where a second reflection and a second transmission occur, and so on. The total reflection and total transmission, respectively $R_{\rm tot}$ and $T_{\rm tot}$, are the sum of reflections ($\propto I_r^x$) and transmissions ($\propto I_o^x$) occurring at different orders x. The difference between the initial and final intensities corresponds to the absorbed light component.

thus it propagates through materials of different refractive indexes. Therefore, besides the radiation absorbed by the acrylic, a fraction of incoming light is lost because of the reflection on this boundary surface. In this experiment, we used unpolarized light and $\theta_i \sim 0°$ (so $\theta_t \sim 0°$), thus the reflective coefficient to consider in our case is:

$$R = \left(\frac{n_1 - n_2}{n_1 + n_2}\right)^2 . \tag{4}$$

Reflection occurs every time light passes through a discontinuity between two refractive indexes, as schematically shown in Fig. 8, thus, by considering a real case, one should expect a series of reflections, transmissions and absorptions, as well as a fraction of diffused light. However, the latter will not be considered in these tests because it is assumed that the samples under investigation are homogeneous, so diffused light is negligible.

Therefore, by taking into account the material reflectance and considering the value of incoming light into the sample equal to 1, it will result in an outgoing light equal to

$$T = \frac{I_o}{I_i} = 1 - R_{\rm tot} - {\rm Abs}_{tot} , \tag{5}$$

where the total reflected and absorbed fractions of the incoming light are $R_{\rm tot}$ and ${\rm Abs}_{tot}$, respectively. Since the materials under analysis are transparent and the angle of incidence between the light beam and the sample surfaces is zero, both $R_{\rm tot}$ and ${\rm Abs}_{\rm tot}$ have been implicitly considered in the measurements of T in this study.

The reflected and transmitted rays were collected with the spectrophotometer and both the transmittance and reflectance coefficients of the acrylic materials were measured in order to define the most suitable materials for the mPMT system.

The transmittance measurements were performed in different configurations by placing samples in air and in pure water, and then again in air after coupling the samples with an optical gel in order to take into account the effect induced by the refractive indexes of the different boundary surfaces. The latter configuration is of great interest as the gel should improve the overall transmittance of light, since the final design of the configuration of the mPMT considers optical gel will fill the gap between the PMTs and the acrylic dome performing a better optical continuity (more details are given in Section 4.3).

4.1. Measurements in air

Measurements have been performed by placing each acrylic sample at a time in the S position (see Section 3.1 for S and R positions), whereas the R position was left empty, so that the reference beam was passing through air. Thus, in the comparative analysis of these two transmitted-beam intensities it is assumed 100% transmittance for the reference beam, assuming a negligible absorption of air.

Fig. 9 shows the transmittance results of the different samples, by considering the wavelength interval ranging from 250 nm to 750 nm in steps of 4 nm. Results show that the E5 mm sample has both the highest and the widest transmittance. In fact, it has a transmittance of about 80% down to 288 nm and more than 90% at the 400–750 nm region. In the range between 360 nm and 750 nm the transmittance values are quite stable for most of the samples, while between 320 nm and 360 nm the transmittance reduction is slightly greater in thicker sample. With the exception of the E18 mm sample, only small differences are observed among all samples. At lower wavelengths the trend changes suddenly as the transmittances quickly drop leading to significant differences among the samples. The transmittance of Poly One samples ranges between 3%–43% at about 290 nm, while it sits between 22%–81% in the Evonik ones. At 272 nm, the E5 mm transmittance is around 41% (the double of the E8 mm), whereas for all the other samples it is found to be smaller than 10%, and in some cases even negligible (below 0.01%).

The E18 mm was expected to be UVT, but the measurements show a big discrepancy to the other Evonik samples, indicating that it is not a proper UVT material. Its behavior is significantly different with respect to those of the thinner samples provided by the same company and, in fact, its transmittance falls down as soon as the measurements move into the UV region, starting from about 400 nm. However, it is worth to specify that the E18 mm was not a standard product for Evonik Company, and the high quality of material is guaranteed for thicknesses up to 8 mm. Nevertheless, the E12 mm also performed very well in our tests.

As concerning the absorbance in E18 mm at shorter wavelengths, we emphasize this aspect in order to address possible reasons that would compromise the proper operation of acrylic in experiments where UV transmittance can be fundamental. It is known that acrylic materials can be degraded by light [38,39]. Some additive products are mixed with them to prevent their aging, but UVT acrylics do not have any anti-UV additive. Since this is a critical point to our applications, further measurements are planned to define the correct procedure to handle acrylic components during the mPMTs assembly/transportation phases as well as during their installation in the detector. An example to preserve mPMT transparency and acrylic characteristics could be the use of LED instead of fluorescence room light during the assembly, and dark covers for hosting detectors during the transportation and temporary storage.

We report in Table 3 representative transmittance values from 300 to 400 nm for an easier comparison between the samples characterized in this work and the preliminary transmittance values used as references for the Hyper-K requirements.

4.2. Measurements in water

Measurements in water have been performed with two small slats obtained from the 5 mm-thick and 4.75 mm-thick acrylic sheets to compare the response of these two samples.

Each acrylic sample was prepared by cutting it from the sample sheets to fit it into a 10 × 10 × 45 mm^3 quartz SUPRASIL cuvette by Hellma so that measurements were performed by using the cuvette with the acrylic sample and MilliQ (Merck Millipore) ultra-pure water[6] inside.

Here, the transmittance is obtained by comparing the intensities measured with the samples at different wavelengths with respect to those obtained with the reference sample. For the reference sample, i.e. the cuvette filled with MilliQ ultra-pure water, we assume 100%

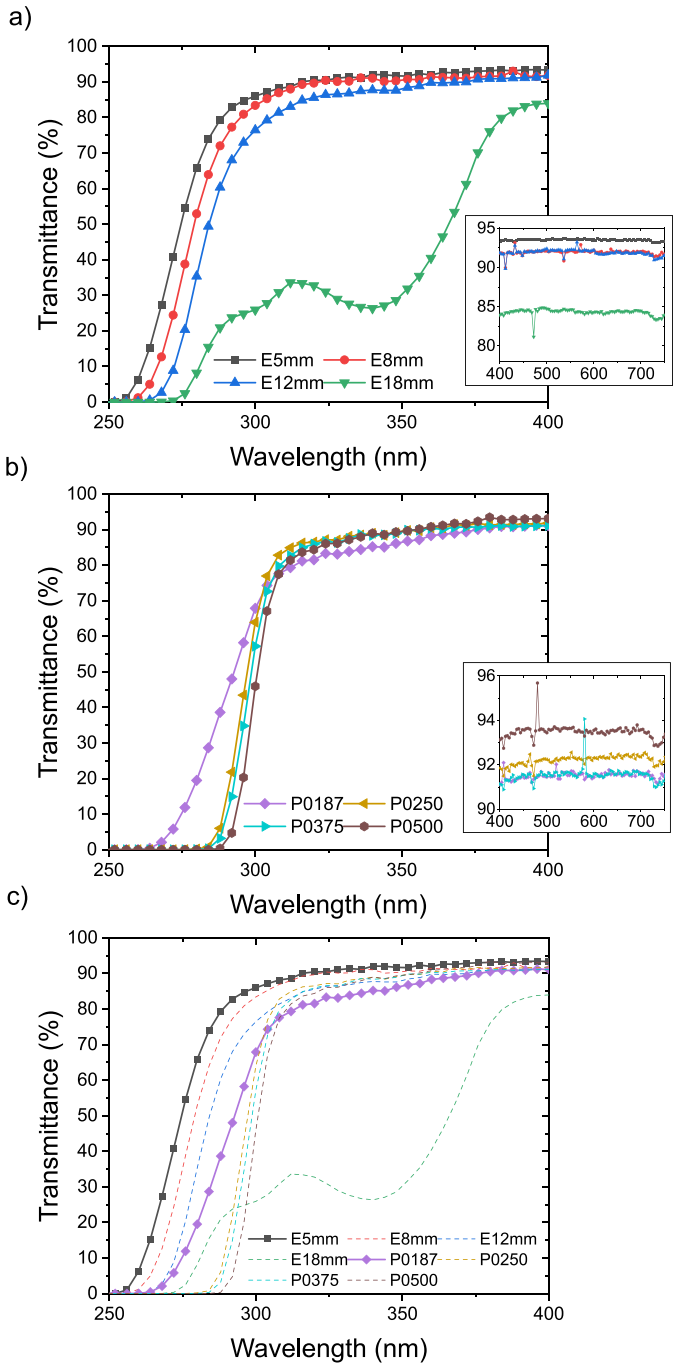

Fig. 9. Transmittance of the 8 samples described in Table 2, collected using the Perkin Elmer Lambda 900 UV/Vis/NIR spectrometer. These results are normalized to the reference beam passing through air. In panel (a), the measurements of the Evonik samples are reported. The bigger plot of the panel shows transmittance in the 250–400 nm range, while the small plot is focused on the 400–750 nm range, where transmittances are comparable among E5 mm, E8 mm and E12 mm, but E18 mm shows some differences also in this range. In panel (b), the measurements of the Poly One samples are reported in the ranges and criteria as described in panel (a). In panel (c), all the eight measurements are displayed together in the 250–400 nm range where differences among samples are mostly pronounced. In particular, the E5 mm and P0187 curves are highlighted (full lines) as the best transmittance values for each sample of their respective company batches; E18 mm shows a significantly poorer transmittance in the UV region of the spectrum when compared to the other samples.

Table 3
The preliminary acrylic Hyper-K transmittance references and the measured transmittances of the E5mm and P0187 samples are reported for wavelengths between 300 and 400 nm. The transmittance reference values are compared with 5 mm-thick samples. The ranges indicate the minimal and maximum acceptable values, but obviously, values greater than the maximum are more than acceptable.

Wavelength (nm)	Transm. ref. min.-max. (%)	E5mm Transm. (%)	P0187 Transm. (%)
300	76.5–83.8	86.0	67.9
310	80.0–86.0	88.4	78.5
320	81.7–87.0	90.4	81.5
325	83.0–87.5	90.6	83.2
340	85.0–89.3	92.0	85.2
350	86.5–90.3	91.7	86.5
360	87.5–91.0	91.9	88.3
375	89.0–92.0	93.0	90.0
380	89.2–92.3	93.1	90.5
400	90.0–93.0	93.3	91.1

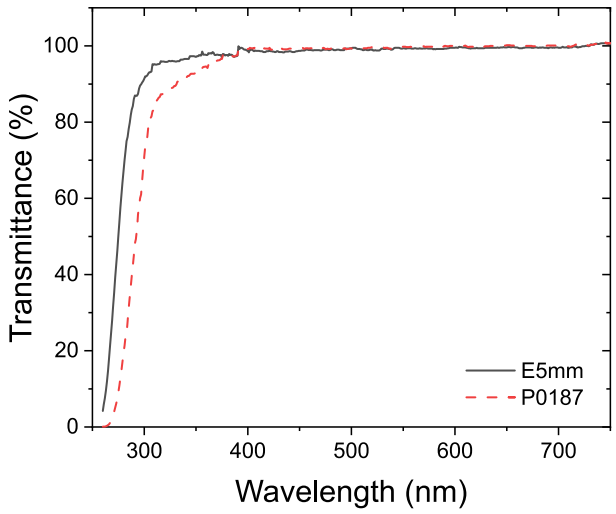

Fig. 10. Measured transmittances of the E5 mm (black solid line) and P0187 (red dashed line) samples in the quartz cuvette filled with MilliQ ultra-pure water. The measures are taken with the 6715 UV/Vis spectrophotometer. The 100% transmittance used as reference is the quartz cuvette filled with MilliQ ultra-pure water.

transmittance. Light beams ranging between 260–800 nm with a step of 1 nm were used for characterizing the samples.

With respect to the reference, the transmittance reduction observed with each acrylic material type inserted in the cuvette filled with ultra-pure water behaves differently for wavelengths in the UV region of the spectrum (≲400 nm) as shown in Fig. 10. On the other hand, both acrylic samples have about 100% transmittance values for wavelengths in the visible range (> 400 nm). The same behavior is expected for the configuration where the acrylic surface of the mPMT dome is immersed in water.

In the P0187 sample, the transmittance decreases faster from under 90% at 330 nm to below 50% at a wavelength of 292 nm when compared to the E5 mm sample, which shows a transmittance dropping from above 90% at 300 nm to under 50% at 275 nm. Therefore, similarly as observed in the air measurements, a higher transmittance can also be achieved in water when using the E5 mm sample.

4.3. Transmittance measurements with acrylic and optical gel

Two acrylics samples obtained from E5 mm and P0187 were coupled each with a 5-mm-thick layer of optical gel laid on one side of

[6] 2 ppb TOC (Total Organic Carbon)

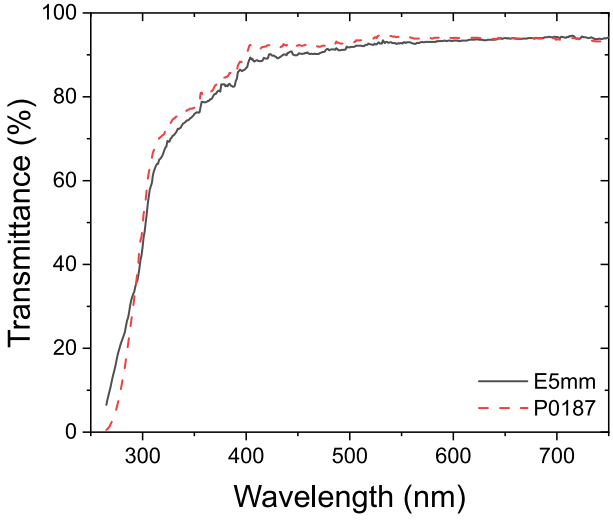

Fig. 11. Transmittance spectra of E5 mm (black solid line) and P0187 (red dashed line) samples with a 5 mm-thick layer of WACKER SilGel® 612 optical gel. The data are acquired by a 6715 Jenway UV/Vis spectrometer.

their surfaces, as explained in Section 2 and the obtained samples are shown in Fig. 4. This configuration has been considered because the gel will be applied to the internal surface of the acrylic dome relative to the mPMT, while the external surface will be in contact with water. Given that the optical gel is not going to be in direct contact with water, the 100% reference transmittance is referred to that in air for this test.

The transmittance graphs of these samples are shown in Fig. 11. The transmittance is about 90%–94% for both samples for wavelengths between 420–750 nm, with the P0187 sample about 1%–2% higher than E5 mm in the 420–570 nm range, but this difference is comparable with the accuracy of the instrument, so the two curves well agree within errors. A reduction in the transmittance starts around 420 nm, where a first drop appears. It then drops at a constant rate until a second drop identified around 315 nm. At this point, the transmittance is about 63% and the slope of the curve becomes steeper, reaching transmittance of less than 30% at about 290 nm. As for the Hyper-K experiment, this reduction in transmittance might not be negligible and can reflect in the effectiveness of the physics analysis studies as it can affect the efficiency in collecting Cherenkov light produced by particles from neutrino interactions in the water tank. For example, considering a PMT candidate by Hamamatsu, the R12199 model[7], the quantum efficiency (QE) ranges between 20% and 30% within ~325 nm and ~425 nm, therefore a better transmittance is recommended in this range. Specifically, at ~350 nm, if PMT QE is ~15% and the acrylic-gel layer has a transmittance of ~76%, then the effective QE of PMT coupled to the acrylic-gel layer results ~11%; whereas, if the acrylic-gel layer has a transmittance of 91%, the effective QE results ~13.5%.

4.3.1. Measurements in water and with optical gel. Further discussions

Transmittance measurements in water and with the acrylic surface covered by a gel layer were performed using the same 6715 Jenway UV/Vis spectrophotometer but with different reference samples. For the acrylic-gel sample, air was used as reference, whereas for the acrylic in water, a cuvette filled with water served as reference. In the latter case, the cuvette filled with water represents 100% transmittance; when the acrylic is placed in the cuvette, it effectively replaces the water volume with acrylic. This implies that when we observe 100% transmission in the test performed in water, the acrylic exhibits transmittance identical to that of the reference sample; in other words, the acrylic is as transparent as water. On the other hand, when the transmittance is less than 100%, then the acrylic transmits less light compared to water. For the E5 mm sample, its transmittance remains between 100% and 95% from 750 nm to ~ 305 nm, and it decreases to 40% at shorter wavelengths down to ~ 270 nm.

On the other hand, although the acrylic-gel transmittance and acrylic transmittance tests were performed using two different instruments, both use air as the reference (i.e., air has 100% transmittance), allowing direct comparison between them. As expected, the sample with only 5 mm-thick acrylic shows higher transmittance than the acrylic-gel sample, since the latter includes 5 mm of gel in addition to the 5 mm of acrylic. However, the comparison between the transmittance spectra of the acrylic and acrylic-gel samples reveals some differences. Specifically, the acrylic-gel spectrum shows a knee at about 400 nm, indicating that the gel has intrinsic absorption between 300 and 400 nm. Despite this drawback, the water-acrylic-gel-PMT system provides better optical uniformity (i.e., smaller refractive angles) than the water-acrylic-air-PMT system. The refractive indices of the materials involved are 1.34–1.50–1.40–1.51 in the first case and 1.34–1.50–1.00–1.51 in the second case, meaning that in the first case the light ray will find a better optical coupling after passing through those materials.

5. Reflectance measurements

As discussed in Section 4, improved light transmission can be achieved not only by reducing absorption within the material through which light propagates but also by minimizing the reflectance between two media with different refractive indices. Another important aspect of the refractive index is that it is a relevant distinctive signature of materials. Consequently, reflectance measurements on the samples described in Table 2 were performed. For these measurements the Perkin Elmer Lambda 900 UV/Vis/NIR spectrometer in reflectance configuration, illustrated in Section 3.1, was used. The comparative measurements were collected simultaneously placing a sample and a reference sample in the S and R positions. An aluminium mirror was the reference sample for these reflectance tests. The relative dependence of the reflectance values of the acrylic samples with wavelengths is reported in Fig. 12. Reflectance varies with the wavelength, sample material, thickness, and the difference between the refractive indices of two adjacent surfaces (Eq. (4)). Specifically, light crossing the interface between two media with different refractive indices can be partially or totally reflected, as mentioned in Section 4 and illustrated in Fig. 8. In measurements described here, light passes through air before and after crossing the transparent sample. This results in a fraction of the light reflecting in the first media interface (air-acrylic), another fraction getting absorbed by the acrylic medium, and ultimately a third part that gets reflected in the second media interface (acrylic-air). A combination that minimizes these three attenuation contributions in media will optimize the overall transmission.

Apart from E18 mm, the measurements reported in Fig. 12 show similar relative reflectance values of approximately 9.0–9.5% for all seven samples between 750 nm and 400 nm. However, differences in reflectance among the samples become more pronounced as the wavelength decreases further at 250–400 nm, namely where the transmittances start to reduce and the samples begin to distinguish. Considering the same material, the differences could be attributed to the varying thicknesses of the samples, given that we used a reflectance accessory with a 6° incident angle. In fact, the second reflection of the incoming beam (i.e., I_r^2 in Fig. 8) might combine with the beam from the first reflection, resulting in the measurement of $I_r^1 + I_r^2$. Since I_r^1 remains constant for the same material, the I_r^2 component should decrease as the sample thickness increases due to greater light absorption in the thicker material. However, as mentioned in Section 3.1, our setup is configured to discard the second reflection when the sample thickness is greater than ~10 mm, meaning that the instrument's light

[7] R12199PMTmodelattheHamamatsuwebsite

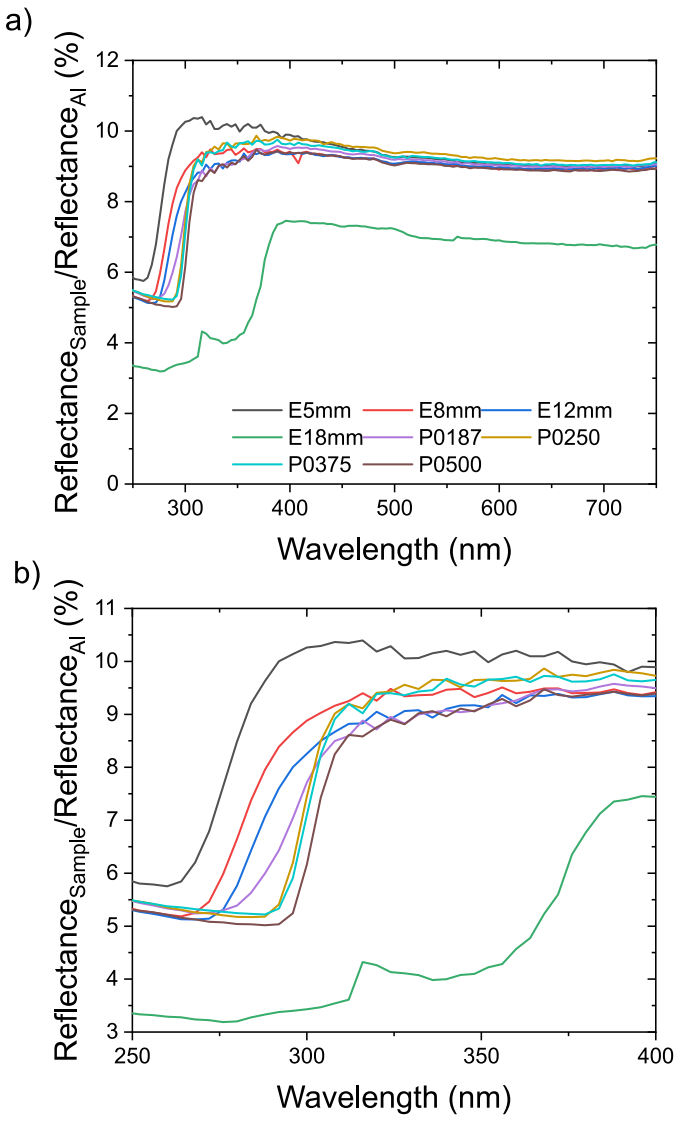

Fig. 12. Reflectance of the 8 samples described in Table 2. In panel (a), the measurements are normalized to the reference beam reflecting on an aluminium mirror, and are collected by using the Perkin Elmer Lambda 900 UV/Vis/NIR spectrometer. Panel (b) shows an inset focused between 250 nm and 400 nm in wavelength axis, and between 3% and 11% in relative-reflectance axis. E18 mm shows a very different behavior with respect the other samples, as in the transmittance test.

detector measures only the first reflection from sample surface in those cases. Thus, the reflection I_r^2 may be detected for the thinner samples, i.e., E5 mm, E8 mm, P0187, P0250 and P0375. Theoretically, for samples from the same company, having the same composition, deviating only in their thicknesses, we would expect similar reflectance curves, having the same shape but slightly shifted, since the thinner sample has higher reflection contribute. However, if the manufacturing processes of the same companies depends on the material thickness, the corresponding reflectance curves will have different shapes, as shown with our measurements.

As shown in panel (b) of Fig. 12, the reflectance curves of the E8 mm and E12 mm Evonik samples have the same shape, even if the E8 mm has a greater intensity close to and over the UV range as expected for the previous discussion. This indicates consistent composition and manufacturing procedures. The variation in reflectance observed between the E5 mm sample and the E8 mm and E12 mm samples is more pronounced, suggesting some differences between their manufacturing conditions or compositions. This is consequence of the fact that E5 mm does not have only a higher reflectance for its thickness (such as E8 mm with respect to E12 mm), but also because of a different shape. Finally, the reflectance curve of the E18 mm sample is significantly different from those of the other Evonik samples, corroborating the transmittance results, and this suggests that the E18 mm sample may have been produced using different procedures and/or compositions, or it may have been deteriorated, for example because of a prolonged light exposure. On the other hand, as regarding the Poly One samples, the P0250 and P0375 samples exhibit similar reflectance curves, especially in the 250–400 nm range, hence the samples were likely realized with identical, or very similar, compositions and procedures. In this case, the reflectance values of these two samples are more similar with respect to the ones of the E8 mm and E12 mm samples, because they absorb more light in the UV range, so that the secondary reflection is more negligible in Poly One samples than for the Evonik samples. The P0500 sample shows a very similar response to the previous two comparing their curve, indicating similar manufacturing procedures and composition, but reflection is less intensive because its I_r^2 component is not combined with I_r^1 and, thus, not detected. Finally, the P0187 sample's reflectance curve is practically overlapped with P0500 sample up to 310 nm, after which it diverges for shorter wavelengths by changing in slope, and indicating a possible variation during its manufacture.

Within the instrumental errors (i.e., ± 0.08 nm in UV/Vis range and $\pm 0.08\%$ in the relative reflectance measures), the reflectance results have pointed out differences among these samples because of their different refractive indeces, and this may depend on differences in the chemical and/or physical properties of those samples. Thus, even if one could expect equal spectral indeces among samples from the same company, some difference in manufacturing procedures and/or in composition of the acrylic mixtures may be present. It is worth mentioning that we can exclude the possibility that sample preparation damaged or altered the E18 mm material, as the same preparation process was used for all samples, none of which show similar behaviors. Additionally, any heating during the cutting process cannot account for alterations in the midpoint of the sample (approximately 2.5 cm from the cutting site) since the temperature was mild enough to handle the samples immediately after cutting.

In summary, although reflectance measurements alone are not sufficient for selecting the optimal acrylic material for our application, they are valuable for detecting significant alterations. Variations in reflectance may indicate changes in the material's refractive index, suggesting modifications either within the material itself or on its surface (e.g., residual glue from protective films). Therefore, performing reflectance optical measurements on each acrylic batch during the mPMT mass-production phase is recommended as a quality control measure for the acrylic window.

6. Photoluminescence measurements

Photoluminescence (PL) emission of a material depends on its intrinsic characteristics, the presence of possible impurities, or external agents that can change its chemistry and physics properties. In experiments such as Hyper-K, the contamination by light sources neither required nor expected can generate unwanted photons (noise) to signals arising from Cherenkov radiation produced by particles from neutrino interactions in the HK water tank. The PL phenomenon also applies to acrylic materials [40,41], thus an analysis of the PL has been undertaken on an acrylic-based glue proposed for the mPMT closure system, in order to study its spectrum of the light from PL emission.

While certain acrylic glues are a practical and cost-effective choice for bonding the two hemispheres of the mPMT acrylic domes, opting for a particular adhesive is contingent upon experimental requirements. Relevant features considered for the test setup are both the luminous noise contributing to the total background noise, and the damage due to the glue-curing procedure on the other mechanical elements and on the entire instrumentation of the mPMTs. In fact, the closure of the vessel is

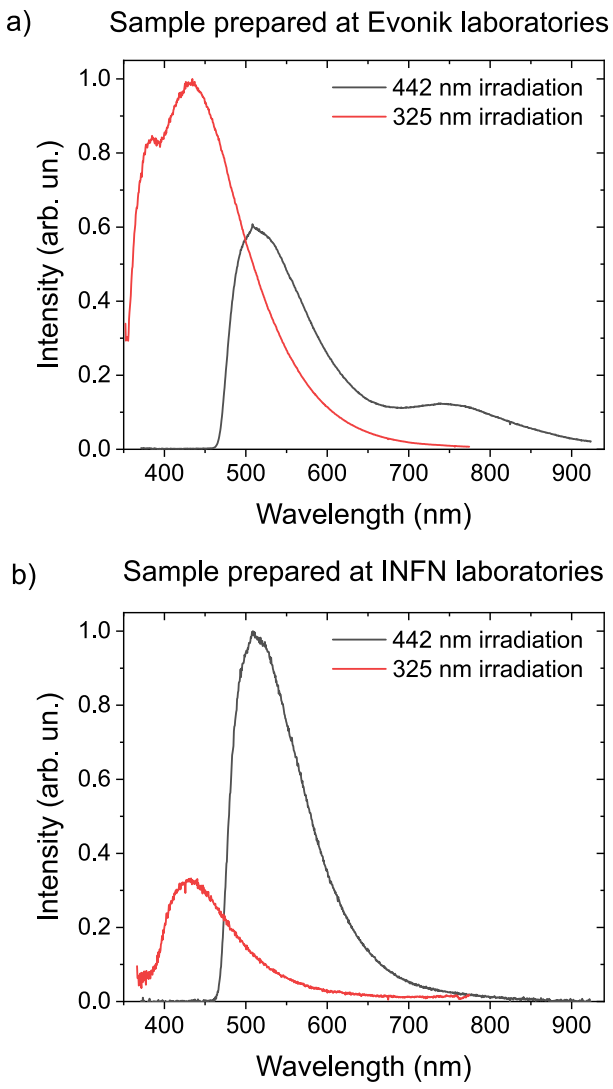

Fig. 13. Photoluminescence spectra of the glue samples by using the two lines (λ_1= 325 nm and λ_2 = 442 nm) of a HeCd laser as excitation source. The samples in the (a) and (b) panels were prepared at Evonik and at INFN-Naples laboratories, respectively. The measured intensity is in arbitrary units and normalized to the respective maximum-peak values in each plot, at 432 nm and 513 nm.

the last step in a mPMT assembly after all other components have been already installed. Some glue curing process cannot proceed naturally but rather happen by exposing the glue mixing to UV irradiation or heating for an extend period of time. Either of these two processes has the potential to affect the operation of the mPMT photosensors, because an intense UV exposure can generally reduce the sensitivity of bialkali photocathodes and speed its aging up (e.g., [42–44]), while the curing temperature can damage PMT if greater than the storage temperature (e.g., −30 °C to +50 °C for the R14374 PMT model by Hamamatsu company). Taking this into consideration, only acrylic glues which do not need heat or UV irradiation to cure have been considered. Besides, a plan has been developed to minimizes risks to components during the mPMT assembly.

The two samples under test and the experimental setup are described in Section 2 and Section 3.2, respectively. The results are reported in Fig. 13. In particular, when irradiated with 325 nm laser, the PL emissions are present in the UV–Vis area. In panel (a) of Fig. 13, the sample produced at Evonik labs shows a two-peak structure in the UV–Vis region, with a main peak at 450 nm and the second at ∼380 nm. However, the latter peak might be an artifact introduced by the use of the high-pass filter mentioned above. In fact, the peak-like shape at 380 nm may represent a residual emission partially cut off by the filter, resulting in undetected contributions to the PL emission at lower wavelengths. When using the 442 nm laser line, a strong peak emission can be observed in both samples at around 525 nm with a tail extending into the near-infrared range (black lines in the graphs). In this region, the Evonik sample shows a second emission peak, centered at around 750 nm, contrary to the INFN sample where this peak is absent, as shown in panel (b) of Fig. 13.

The significance of the results from the PL tests reported here is that, despite the differences between the samples prepared at Evonik and at INFN laboratories, both show two dominant peaks around 510 nm and 430 nm, if irradiated by light at 325 nm and 442 nm, respectively. This means that the PL of this glue has intrinsic responses activated by the two frequencies of the laser, though those peaks emit with inverted intensities between the two samples. In other words, secondary photons in the UV and Vis regions of the spectrum were generated by PL with different features from each sample, that might not be completely removed also with other combinations of the two components of the glue and other indications reported in the data sheet.

Although this kind of glue is safe for the mPMT assembly and for its components since its curing does not need neither UV irradiation nor heating, its use in an experiment requiring low-luminosity background without a proper study of its impact to the physics goals of the experiment would not be wise. Both samples, in fact, absorb photons in the UV range and emit PL light with longer wavelengths sitting in the sensitivity range of the PMTs that will instrument the HK. Giving that the Cherenkov effect is the principal process used to detect particles interacting in the Hyper-K experiment, the PL properties of the studied glue might contribute to increase the background noise level. The results of this study, then, indicate that the use of this glue for closing and sealing the vessel might not be an appropriate solution, while it could be difficult to find commercially available acrylic-based glues with minimal or non-existent PL properties [45]. Consequently, a more complex solution, based on a mechanical closure is strongly recommended to assemble the mPMTs. Further details concerning prototypes based on a mechanical closure can be found in [24,27].

7. Conclusions

The identification of weak and rare events expected from neutrino interactions in the water of the Hyper-K experiment, currently under construction, requires extremely high resolution, efficiency, and exceptionally low levels of radioactive contamination and emanation from all the items that will be used in HK, therefore the mPMT optical module must be in compliance with all these requirements. To be compliant with these constrains is crucial to achieve the highest possible signal-to-noise ratio and enable detections at low energy levels. Additionally, the mPMT design must ensure reliability for over 20 years, as required in HK, while using non-degrading materials that maintain water quality and avoid any effects that might affect light transmission. The selection of materials to guarantee optimal and safe operational conditions for the optical units that will instrument the next generation of large-scale experiments motivated this work. Protective cases and vessels for underwater optical units must provide a dry, controlled environment to maintain the integrity and optimal functionality of electronic components. These enclosures also need to offer maximum transparency for efficient light detection, extending into the UV region where most Cherenkov photons are emitted. The high costs associated with ultra-pure glass make it an impractical choice. Instead, the acrylic materials considered in this study exhibit desirable properties that make them suitable for use in HK: (i) low intrinsic radioactivity, (ii) affordability and ease of molding, (iii) optical transparency, and (iv) mechanical stability under high pressure.

We present the optical characterization of different acrylic materials intended for use as domes and of an optical gel used for optical coupling between the acrylic domes and the PMTs to enhance the overall

transmittance in the assembly of the HK mPMT vessel. The higher transmittance observed in the UV range suggests that the E5 mm, E8 mm, and E12 mm samples from Evonik are suitable acrylic candidates for our purposes. A key goal of this study was to demonstrate that high-quality, UV-transparent commercial acrylics can achieve transmittance levels comparable to the ones of preliminary references for Hyper-K and reported in the second column of Table 3. This opens the possibility of collaborating with manufacturers to obtain the best material under favorable conditions. This study also included reflectance measurements, revealing that reflectance varies with sample thickness, but suggesting that the optical properties of the acrylic sheets may be influenced by the manufacturing process as well. This approach provides crucial information for quality assurance of materials used in the mPMT assembly during mass production. To ensure optimal performance of each mPMT, the transmittance and reflectance of each acrylic batch selected for mass production must undergo thorough quality control.

A suitable refractive index for the optical gel is a widely used solution to ensure the high transmittance needed for efficient photon detection. This is achievable when the gel's refractive index closely matches that of both the acrylic and the PMT photocathode glass cover, with an intermediate index between these two materials being ideal. Additionally, gel with intrinsically high transmittance in the UV–Vis range is beneficial to avoid significantly limiting the performance of the acrylic dome.

As regarding the photoluminescence tests done on the two samples made with the same acrylic glue, experimental results show that both glue samples emit photoluminescence photons, which could potentially impact the HK measurements. Since the Cherenkov effect is the primary process for detecting particles interacting in HK, the PL contribution from the glue might increase noise levels and reduce the quality and precision of the Hyper-K measurements. As a result, glue was avoided, and a mechanical solution was adopted to close and seal the vessel domes for prototyping. This approach was successfully validated through pressure and sealing tests. The mechanical closure also offers the advantage of allowing the reopening of mPMT vessels after assembly without damaging or breaking the acrylic domes. This feature enables access for repairs to any damaged components within an mPMT.

Although experimental requirements necessitated significant modifications to the final mPMT vessel design, the study described in this paper supported the international Hyper-K community in adopting acrylic and gel materials for the mPMT pressure vessel and corroborating its installation in HK. Furthermore, in a larger view, our findings highlight and leverage the advantages of plastic materials for this type of experiments.

CRediT authorship contribution statement

Alan Cosimo Ruggeri: Writing – review & editing, Writing – original draft, Methodology, Investigation, Data curation, Conceptualization. **Riccardo Funari:** Writing – review & editing, Writing – original draft, Investigation, Data curation, Conceptualization. **Deborah Katia Pallotti:** Writing – review & editing, Writing – original draft, Investigation, Data curation, Conceptualization. **Antonio Di Nitto:** Writing – review & editing, Writing – original draft. **Bartolomeo Della Ventura:** Writing – review & editing, Investigation. **Aurora Langella:** Writing – review & editing. **Lucas Nascimiento Machado:** Writing – review & editing. **Davide Bianco:** Writing – review & editing. **Luigi Lavitola:** Visualization. **Alfonso Boiano:** Writing – review & editing, Visualization. **Alessandro Di Nola:** Writing – review & editing. **Maria De Luca:** Writing – review & editing. **Ciro Riccio:** Writing – original draft, Visualization. **Raffaele Velotta:** Writing – review & editing, Resources. **Pasqualino Maddalena:** Writing – review & editing, Resources, Investigation, Conceptualization. **Gianfranca De Rosa:** Writing – review & editing, Resources, Investigation, Funding acquisition, Conceptualization.

Declaration of competing interest

The authors declare the following financial interests/personal relationships which may be considered as potential competing interests: Alan Cosimo Ruggeri reports financial support and travel were provided by Horizon Europe (JENNIFER2 - Japan and Europe Network for Neutrino and Intensity Frontier Experimental Research 2). Alfonso Boiano reports travel was provided by Horizon Europe (JENNIFER2 - Japan and Europe Network for Neutrino and Intensity Frontier Experimental Research 2). Gianfranca De Rosa reports travel was provided by Horizon Europe (JENNIFER2 - Japan and Europe Network for Neutrino and Intensity Frontier Experimental Research 2). Aurora Langella reports travel was provided by Horizon Europe (JENNIFER2 - Japan and Europe Network for Neutrino and Intensity Frontier Experimental Research 2). Luigi Lavitola reports travel was provided by Horizon Europe (JENNIFER2 - Japan and Europe Network for Neutrino and Intensity Frontier Experimental Research 2). If there are other authors, they declare that they have no known competing financial interests or personal relationships that could have appeared to influence the work reported in this paper.

Acknowledgments

This work was supported by the Horizon 2020 Marie Sklodowska-Curie RISE project JENNIFER2, Grant Agreement No. 822070. Authors thank the Evonik IndustriesAG (now become Röhm GmbH) and Poly One Corporation for providing the acrylics samples. We acknowledge the workshop of INFN-Naples, in particular Mr. Franco Cassese and Mr. Benedetto De Fazio. We also acknowledge the KM3NeT group of INFN-Naples for its availability, in particular, Mr. Raffaele Rocco for his support for preparation of the optical-gel samples. Many thanks to Mr. Maurizio Mongelli for his drawings, his precious help concerning the mPMT design, all his suggestions and discussions. This work has been performed in the context of the Hyper-Kamiokande collaboration and is supported by its membership.

Data availability

No data was used for the research described in the article.

References

[1] Y. Totsuka, Super-kamiokande, 1990, (Univ. of Tokyo) Report No. ICRR-227-90-20.
[2] S. Fukuda, Y. Fukuda, T. Hayakawa, et al., The super-kamiokande detector, Nucl. Instrum. Methods Phys. Res. A 501 (2) (2003) 418–462.
[3] K. Abe, Y. Hayato, T. Iida, et al., Calibration of the super-kamiokande detector, Nucl. Instrum. Methods Phys. Res. A 737 (2014) 253–272.
[4] T2K Collaboration, K. Abe, J. Adam, et al., T2K Collaboration Collaboration Collaboration, Observation of electron neutrino appearance in a muon neutrino beam, Phys. Rev. Lett. 112 (2014) 061802.
[5] K. Abe, R. Akutsu, A. Ali, et al., Constraint on the matter–antimatter symmetry-violating phase in neutrino oscillations, Nat. 580 (7803) (2020) 339–344.
[6] K. Abe, T. Abe, H. Aihara, et al., Letter of intent: The hyper-kamiokande experiment — Detector design and physics potential —, 2011.
[7] Hyper-Kamiokande Proto-Collaboration, K. Abe, H. Aihara, et al., Physics potential of a long-baseline neutrino oscillation experiment using a J-PARC neutrino beam and hyper-kamiokande, Prog. Theor. Exp. Phys. 2015 (5) (2015) 053C02.
[8] I.E. Tamm, I.M. Frank, Visible emission of clean liquids by action of γ radiation, Dokl. Akad. Nauk. SSSR 14 (107) (1937).
[9] P.A. Čerenkov, Visible emission of clean liquids by action of γ radiation, Dokl. Akad. Nauk. SSSR 2 (451) (1934).
[10] S. Adrián-Martínez, M. Ageron, F. Aharonian, et al., Deep sea tests of a prototype of the KM3net digital optical module, Eur. Phys. J. C 74 (2014) 3056.
[11] Gianfranca De Rosa, A multi-PMT photodetector system for the hyper-kamiokande experiment, Nucl. Instrum. Methods Phys. Res. A 958 (2020) 163033, Proceedings of the Vienna Conference on Instrumentation 2019.
[12] Aurora Langella, A multi-PMT photodetector system for the hyper-kamiokande experiment, Nucl. Instrum. Methods Phys. Res. A 1052 (2023) 168275.

[13] Gianfranca De Rosa, A multi-PMT photodetector system for the hyper-kamiokande experiment, PoS ICHEP2020 (2021) 831.
[14] Yasuhiro Nishimura, New large aperture photodetectors for water cherenkov detectors, Nucl. Instrum. Methods Phys. Res. A 958 (2020) 162993, Proceedings of the Vienna Conference on Instrumentation 2019.
[15] C. Bronner, Y. Nishimura, J. Xia, T. Tashiro, Development and performance of the 20" PMT for hyper-kamiokande, J. Physics: Conf. Ser. 1468 (1) (2020) 012237.
[16] A. Suzuki, M. Mori, K. Kaneyuki, et al., Improvement of 20 in. diameter photomultiplier tubes, Nucl. Instrum. Methods Phys. Res. A 329 (1) (1993) 299–313.
[17] K. Abe, Y. Hayato, T. Iida, et al., Calibration of the super-kamiokande detector, Nucl. Instrum. Methods Phys. Res. A 737 (2014) 253–272.
[18] Kamioka Observatory, ICRR (Institute for Cosmic Ray Research), The University of Tokyo, https://www-sk.icrr.u-tokyo.ac.jp/en/hk/pr/https://www-sk.icrr.u-tokyo.ac.jp/en/hk/pr/, https://youtu.be/jfoe3d2z7lm, https://Youtu.Be/JFOE3D2z7LM.
[19] Alan Cosimo Ruggeri on behalf of the Hyper-Kamiokande Collaboration, Hyper-kamiokande detector and its capabilities in astrophysical neutrino search, J. Phys. Conf. Ser. 2429 (1) (2023) 012030.
[20] Jan Kisiel, Photodetection and electronic system for the hyper-kamiokande water cherenkov detectors, Nucl. Instrum. Methods Phys. Res. A 1055 (2023) 168482.
[21] Yasuhiro Nishimura, New 50 cm Photo-Detectors for Hyper-Kamiokande, PoS ICHEP2016 (2017) 303.
[22] Y. Kudenko, A. Khotjantsev, O. Mineev, N. Yershov, Development and tests of WLS plates for outer detector of hyper-kamiokande, Nucl. Instrum. Methods Phys. Res. A 1045 (2023) 167543.
[23] Stephane Zsoldos, The outer detector (OD) system for hyper-kamiokande experiment, PoS ICHEP2020 (2021) 886.
[24] Alan Cosimo Ruggeri, R&D studies of new photosensors for the hyper-kamiokande detector, in: Zhen-An Liu (Ed.), Proceedings of International Conference on Technology and Instrumentation in Particle Physics 2017, Springer Singapore, Singapore, 2018, pp. 325–328.
[25] Roberto Spina, Luigi Tricarico, Vincenzo Berardi, et al., Acrylic studies for hyper-kamiokande experiment, Nucl. Instrum. Methods Phys. Res. A 902 (2018) 149–157.
[26] Xiongxin Dai, Etienne Rollin, Alain Bellerive, et al., Wavelength shifters for water cherenkov detectors, Nucl. Instrum. Methods Phys. Res. A 589 (2) (2008) 290–295.
[27] Hyper-Kamiokande Proto-Collaboration, K. Abe, Ke. Abe, et al., Hyper-kamiokande design report, 2018, arXiv:1805.04163.
[28] M. Laubenstein, M. Hult, J. Gasparro, et al., Underground measurements of radioactivity, Appl. Radiat. Isot. 61 (2) (2004) 167–172, Low Level Radionuclide Measurement Techniques - ICRM.
[29] K. Rielage, M. Akashi-Ronquest, M. Bodmer, et al., Update on the miniclean dark matter experiment, Phys. Procedia 61 (2015) 144–152, 13th International Conference on Topics in Astroparticle and Underground Physics, TAUP 2013.
[30] M.G. Boulay, the Deap Collaboration, DEAP-3600 dark matter search at SNOLAB, J. Phys. Conf. Ser. 375 (1) (2012) 012027.
[31] J. Boger, R.L. Hahn, J.K. Rowley, et al., The sudbury neutrino observatory, Nucl. Instrum. Methods Phys. Res. A 449 (2000) 172–207.
[32] F.P. An, J.Z. Bai, A.B. Balantekin, et al., The detector system of the daya bay reactor neutrino experiment, Nucl. Instrum. Methods Phys. Res. A 811 (2016) 133–161.
[33] JUNO Collaboration, JUNO physics and detector, Prog. Part. Nucl. Phys. 123 (2022) 103927.
[34] H. Tokuno, Y. Murano, S. Kawana, et al., On site calibration for new fluorescence detectors of the telescope array experiment, Nucl. Instrum. Methods Phys. Res. A 601 (3) (2009) 364–371.
[35] L. Agostino, M. Buizza-Avanzini, M. Marafini, et al., Future large-scale water-cherenkov detector, Phys. Rev. ST Accel. Beams 16 (2013) 061001.
[36] T. Patzak, the MEMPHYS collaboration, MEMPHYS: A next generation megaton scale water cherenkov detector in europe, J. Phys. Conf. Ser. 375 (4) (2012) 042055.
[37] Perkin Elmer Instruments LLC, Lambda 800/900 - user's guide, 2001.
[38] B. Littlejohn, K.M. Heeger, T. Wise, et al., UV degradation of the optical properties of acrylic for neutrino and dark matter experiments, J. Instrum. 4 (09) (2009) T09001.
[39] Karollyne Gomes de Castro Monsores, Anderson Oliveira da Silva, Susane de Sant' Ana Oliveira, João Gabriel Passos Rodrigues, Ricardo Pondé Weber, Influence of ultraviolet radiation on polymethylmethacrylate (PMMA), J. Mater. Res. Technol. 8 (5) (2019) 3713–3718.
[40] Yann Molard, Frederick Dorson, Konstantin A. Brylev, et al., Red-NIR luminescent hybrid poly (methyl methacrylate) containing covalently linked octahedral rhenium metallic clusters, Chem. Eur. J. 16 (19) (2010) 5613–5619.
[41] R. Sosa Fonseca, M. Flores, R. Rodriguez T., J. Hernández, A. Muñoz F, Evidence of energy transfer in Er3+-doped PMMA-PAAc copolymer samples, J. Lumin. 93 (4) (2001) 327–332.
[42] A. Breskin, CsI UV photocathodes: History and mystery, Nucl. Instrum. Methods Phys. Res. A 371 (1–2) (1996) 116–136.
[43] B.K. Singh, E. Shefer, A. Breskin, R. Chechik, N. Avraham, CsBr and CsI UV photocathodes: new results on quantum efficiency and aging, Nucl. Instrum. Methods Phys. Res. A 454 (2) (2000) 364–378.
[44] A.S. Tremsin, S. Ruvimov, O.H.W. Siegmund, Structural transformation of CsI thin film photocathodes under exposure to air and UV irradiation, Nucl. Instrum. Methods Phys. Res. A 447 (3) (2000) 614–618.
[45] G.R. Araujo, T. Pollmann, A. Ulrich, Photoluminescence response of acrylic (PMMA) and polytetrafluoroethylene (PTFE) to ultraviolet light: Limits on low-intensity photoluminescence in support materials of rare-event search experiments, Eur. Phys. J. C 79 (8) (2019).